APPLIED AND ENVIRONMENTAL MICROBIOLOGY, Feb. 1995, p. 741–748 Vol. 61, No. 2
0099-2240/95/$04.00+0

Bacterial Growth on Surfaces: Automated Image Analysis for Quantification of Growth Rate-Related Parameters

SØREN MØLLER,[1] CLAUS S. KRISTENSEN,[1] LARS K. POULSEN,[1]
JENS M. CARSTENSEN,[2] AND SØREN MOLIN[1]*

Department of Microbiology[1] and Institute of Mathematical Modelling,[2]
The Technical University of Denmark, DK-2800 Lyngby, Denmark

Received 8 September 1994/Accepted 9 December 1994

A fast routine method for estimating bacterial cell growth rates by using the metachromatic dye acridine orange is described. The method allows simultaneous estimates of cellular RNA and DNA contents of single cells. Acridine orange staining can be used as a nonspecific supplement to quantitative species-specific hybridizations with fluorescence-labelled ribosomal probes to estimate the single-cell concentration of RNA. By automated analysis of digitized images of stained cells, we determined four independent growth rate-related parameters: cellular RNA and DNA contents, cell volume, and the frequency of dividing cells in a cell population. These parameters were used to compare physiological states of liquid-suspended and surface-growing *Pseudomonas putida* KT2442 in chemostat cultures. The major finding is that the correlation between substrate availability and cellular growth rate found for the free-living cells was not observed for the surface-bound cells; in contrast, the data indicate an almost constant growth rate for attached cells which was independent of the dilution rate in the chemostat.

Phylogenetic studies of rRNA sequence variations among organisms (58) have made it possible to design phylogenetic stains (13) targeting different groups or species of bacteria (1, 2, 20, 54). Phylogenetic probes targeting the rRNA have been widely used for in situ identification of specific groups of organisms, and they have been useful for description of the spatial distribution of bacteria in multispecies natural populations such as sewage sludge (41), biofilms (39, 40), and the rumen (50).

In natural environments the majority of bacteria grow in complex consortia of microorganisms associated with surfaces (9, 55) referred to as biofilm communities (34). These mixed microbial communities are important ecological systems consisting of numerous species of bacteria (57). Biofilms thicker than a few cell layers often exhibit complex three-dimensional structures (31), and they may contain local microenvironments in which growth conditions are very different from those of the surroundings (10). Therefore, heterogeneity with respect to the physiological states of the organisms present in various microenvironments is to be expected. One way of obtaining an indication of the metabolic activity of these organisms is to measure their respiratory activity. Chemical redox dyes such as 5-cyano-2,3-ditolyl tetrazolium chloride (43) and 2-(*p*-iodophenyl)-3-(*p*-nitrophenyl)-5-phenyltetrazolium chloride (60) have been used as indicators of actively respiring cells in natural systems. The dye rhodamine 123 has also been used as a viability indicator, since this dye is taken up only by cells having active membrane transport (36). These chemical stains provide indications of the proportion of viable cells in a natural sample, but they neither indicate the degree to which the organisms are active nor inform about the overall physiological state of the cells. However, staining of cellular macromolecules with acridine orange (AO) has been used to monitor physiological activity of *Escherichia coli*, i.e., a greater proportion of orange fluorescing cells over green fluorescing cells has been observed for fast-growing cell populations because of high contents of RNA (3). Alternatively, direct cell growth rates may in some cases be estimated from rRNA determinations obtained by quantitative hybridization with ribosomal probes (11). Growth rate estimates on the basis of macromolecular contents have their origin in early observations in microbial physiology. In 1958 Schaechter et al. (45) described the macromolecular composition of *Salmonella typhimurium* when growing in different media, and they found that the content of RNA in a bacterial cell is strictly dependent on the growth rate. It has been demonstrated for several organisms that, at least at higher growth rates, there is a tight correlation between RNA content and growth rate (6, 26, 27, 37, 38, 44). New methods using hybridization with fluorescence-labelled oligonucleotide probes targeting rRNA and microscopy coupled with digital imaging allow estimations of the amount of rRNA probe bound within a single cell, whereby the staining intensity can be related to the bacterial growth rate (11, 39).

Starved organisms contain small numbers of ribosomes (16, 21), as do slowly growing cells. Therefore, using rRNA content as the sole indicator of the physiological states of cells in complex natural systems may, in the presence of starved or nongrowing bacteria, give misleading results. Another inherent problem of the in situ hybridization technique is the quantification of the light emitted from the fluorescent cells when they are examined by digital image analysis. Traditionally, digitized images are analyzed by manually circumscribing individual cells with a pointing device (mouse) and measuring the accumulated intensity from the defined area. This method is highly dependent on the operator, and even for one operator the variation between consecutive measurements is considerable. Also, this method is labor-intensive, allowing only a limited number of cells to be circumscribed and thus making the generation of statistics almost impossible. Approaches to limit these drawbacks have been to employ various automatic global thresholding or edge detection techniques to define cells in a digital image (4, 46, 56), all of which have disadvantages as

* Corresponding author. Mailing address: Department of Microbiology, The Technical University of Denmark, Building 221, DK-2800 Lyngby, Denmark. Phone: 45 45 93 34 22. Fax: 45 45 88 73 28. Electronic mail address: sm@lm.dtu.dk.

discussed below. An alternative procedure is the segmentation algorithm described by Dubuisson et al. (15).

In this communication we report the development of an automated image analysis program which makes it possible to quantify accurately and reproducibly the amount of light emitted from a single cell. The analysis of the digitized images also allows the determination of other growth rate-related parameters, such as cell volume and the frequency of dividing cells (FDC). The FDC has been used as an indicator of biological activity in aquatic communities (23), and it can serve to validate the rRNA and volume measurements. Furthermore, we present a method for a simultaneous quantitative staining of RNA and DNA by using the metachromatic dye AO. Based on the growth rate variation of these macromolecules, this staining method can be used as a fast and convenient indicator of the physiological state of the cell. In the present paper this combination of growth rate-related parameters is used to estimate the physiological state of surface-associated and planktonic cells of the *Pseudomonas putida* strain KT2442.

MATERIALS AND METHODS

Strains and growth media. The strain *P. putida* KT2442 (12) was used in all growth experiments. The growth medium in all batch cultures was AB minimal medium (8) supplied with 6 mM sodium citrate as a carbon source.

Chemostat cultures. Continuous chemostat cultures were grown in AB minimal medium with 3 mM sodium citrate as the sole carbon source at a constant temperature (25°C). The chemostat consisted of a glass cylinder (2.7 cm in diameter) with rubber stoppers at each end. Sufficient stirring was obtained with an air inlet in the bottom of the chamber. A constant volume (approximately 50 ml) was controlled by monitoring the level of the outlet tube at the top of the glass cylinder. To prevent attachment of the bacteria to the inner surface of the chemostat, it was treated with 4% dimethyl-dichlorosilan (Sigma Chemicals, St. Louis, Mo.) and placed in a 110°C oven for at least 1 h before sterilization. To obtain a balanced culture, the chemostat cultures were grown for approximately 10 generations with a constant optical density at 450 nm prior to sampling for hybridization and flow cytometry. Subsequently a sterilized microscope coverslip was introduced into the chemostat, and a surface culture was allowed to develop on this surface for 14 to 18 h before a surface sample and a sample from the liquid phase were fixed for hybridization. The coverslips were cleaned in chloroform, methanol, acetone, and chloroform again (1 min each) before sterilization.

Oligonucleotide probes. Oligonucleotide probes were synthesized with an automatic DNA synthesizer, and an aminohexyl linker (Aminolink 2; Applied Biosystems, Foster City, Calif.) was attached at the 5′ terminus by using a standard DNA synthesis cycle. For hybridizations the probe EUB338, specific for the bacterial domain, was used (49). The probe was labelled with tetramethylrhodamine isothiocyanate (Molecular Probes, Eugene, Oreg.) or the isothiocyanate derivative CY3 or CY5 (Biological Detection Systems, Pittsburgh, Pa.) and purified by reverse-phase liquid chromatography as previously described (30).

Hybridization of whole cells. Samples for hybridization were fixed in 3% paraformaldehyde as previously described (39). For hybridization of single cells (from the chemostat liquid cultures) samples were applied to a poly-L-lysine (Sigma Chemicals)-coated slide (slides were cleaned in 1% HCl in 70% ethanol, dipped into a 0.01% poly-L-lysine solution, and air dried) and dried by sequential washes in 50, 80, and 96% ethanol (3 min each). Subsequent to the ethanol washing 10 μl of hybridization mixture (30% formamide, 0.9 M NaCl, 100 mM Tris [pH 7.2], 0.1% sodium dodecyl sulfate [SDS]) containing 25 ng of probe was added to each hybridization well. Cells were incubated with hybridization solution for 16 h at 37°C in a moisture chamber (49). For washing, the slides were submersed in 100 ml of the following washing solutions. First, the slides were washed in washing solution I (30% formamide, 0.9 M NaCl, 100 mM Tris [pH 7.2], 0.1% SDS) for 20 min at 37°C. Then they were transferred to a 4′,6-diamidino-2-phenylindole (DAPI) staining solution (0.1 M Tris [pH 7.2], 0.9 M NaCl, 6.25 μM DAPI) for 5 min at 21°C, and subsequently they were washed for 15 min in washing solution II (0.1 M Tris [pH 7.2], 0.9 M NaCl) at 37°C, before a final rinsing in 100 ml of distilled water.

To fix the surface-associated cells on glass surfaces, the coverslips were first rinsed in phosphate-buffered saline (PBS; 130 mM NaCl in 10 mM $NaPO_4$ buffer [pH 7.2]) and then fixed overnight in 3% paraformaldehyde in a 50-ml plastic container. The following day the fixative was removed, and, still in the container, the coverslip was washed for 5 min with PBS and then briefly rinsed with 0.1% Nonidet P-40 (Sigma Chemicals) before dehydration in an ethanol washing sequence (50, 80, and 96%; 3 min each). The fixed cells were stored at 4°C in an evacuated dessiccator with silica gel beads. To hybridize the surface samples, a small piece of the coverslip was broken off and placed on a slide for hybridization. The hybridization was performed under the conditions mentioned above, with the modification that the DAPI staining and the washing steps were carried out directly on the slide with 40 μl of each solution.

AO staining. The AO staining was performed directly on paraformaldehyde-fixed cells in AO staining buffer containing EDTA (5 mM EDTA, 0.15 M NaCl, 0.1 M phosphate-citrate buffer [pH 6]) to ensure preferential denaturation of double-stranded RNA inside the cells (53). Samples were applied to poly-L-lysine-coated slides dehydrated as described above and incubated in the dark at room temperature for 5 min with 40 μl of staining solution (22 μM AO in AO staining buffer filtered though a 2.0-μm-pore-size filter to remove AO crystals). The staining solution was removed by a short rinse with distilled water, and the cells were submersed for 30 s in distilled water and rapidly air dried. To remove the RNA in whole cells, 10 μl of concentrated RNase solution (500 to 1,000 U/ml) was added directly to the fixed cells on the slide and they were incubated for 20 to 30 min at 37°C prior to AO staining.

Flow cytometry. Samples for flow cytometry were removed from the balanced chemostat culture and fixed in 70% ethanol as previously described (21). The DNA-specific fluorescence in a sample was normalized to the fluorescence of a sample of *P. putida* KT2442 starved for 4 days. Since a starved culture of *P. putida* KT2442 is assumed to contain one chromosome per cell (21), the number of chromosomes in growing cells could be estimated.

Microscopy. Hybridized and stained samples were analyzed by use of a Carl Zeiss Axioplan epifluorescence microscope. The excitation source was a 100-W HBO bulb or a 75-W XBO bulb (for AO staining), and digital images were captured with a 12-bit cooled slow-scan charge-coupled device camera (KAF 1400 chip; Photometrics, Tucson, Ariz.). The charge-coupled device camera was controlled by using the PMIS software (Photometrics). Generally, the exposure times used were as follows: 80 ms for AO staining of RNA; 500 ms for AO staining of DNA, TRITC, and CY3; and 2,000 ms for CY5-labelled probes. Tetramethylrhodamine isothiocyanate-, CY3-, and CY5-labelled cells were simultaneously stained with DAPI, and the captured images were focused by using filter set 1 (BP 356/12 excitation filter, 395-nm dichroic filter, and LP 397 emission filter) (Carl Zeiss) for DAPI staining to avoid bleaching of the fluorochrome during focusing. Tetramethylrhodamine isothiocyanate CY3, and CY5 were visualized by use of filter sets 15 (BP 546/12 excitation filter, 580-nm dichroic filter, and LP 590 emission filter) (Carl Zeiss), XF40 (BP 560/40 excitation filter, 590-nm dichroic filter, and LP 600 emission filter) (Omega Opticals, Brattleboro, Vt.), and XF45 (BP 610/20 excitation filter, 645-nm dichroic filter, and BP670/40 emission filter) (Omega Opticals), respectively. For AO staining focusing was obtained by using phase contrast, and RNA-specific light was captured by using the XF21 filter set (BP 480/60 excitation filter, 530-nm dichroic filter, and BP635/55 emission filter) (Omega Opticals), while DNA-specific light was captured by using fluorescein isothiocyanate filter set 10 (BP 450-490 excitation filter, 510-nm dichroic filter, and BP515-565 emission filter) (Carl Zeiss).

Image analysis. The amount of light from AO-stained or hybridized cells was quantified by use of the Cellstat image analysis program. For each staining the average intensity of three different images corresponding to between 200 to 500 cells was used. Cellstat is a Unix-based image analysis program capable of handling 16-bit image data. The bases for Cellstat object recognition are cell size (area in pixels) and various shape parameters. A detailed description of Cellstat will be presented elsewhere (unpublished data). At present, on-line information is available on the Internet World Wide Web at the uniform resource locator (URL) http://www.lm.dtu.dk/cellstat/index.html.

By choosing the right parameters for cell identification, it is possible to discriminate between single cells and clumps of cells (Fig. 1A and B). Cell clumps are normally ignored when the average intensity of a planktonic population is calculated, even though an analysis showed that the mean intensities of cell clumps and single cells are equal (data not shown). By using a different set of parameters for object recognition, it is possible to detect and measure the intensities of surface-associated microcolonies (Fig. 1D) and single cells on the surface (Fig. 1C) independently. Thus, Cellstat provides a large amount of flexibility in object recognition. A problem of cell identification by automated image analysis is the determination of the cell edge. Conventional thresholding or manual circumscription for edge identification causes underestimation of the sizes of faint objects, while the sizes of bright objects tend to be overestimated (46). When *P. putida* KT2442 cells are hybridized at different stringencies by using increasing amounts of formamide (from 0 to 70%), the signal intensity decreases approximately sevenfold. Under such conditions the cell areas calculated by Cellstat were constant (data not shown), indicating consistent edge determination regardless of object intensities.

RESULTS

AO staining. The emission spectra of AO upon binding to nucleic acids are highly dependent on substrate structure, i.e., AO complexes with single- and double-stranded nucleic acid will emit red and green fluorescence, respectively (42). This provides the basis for using AO to simultaneously stain RNA and DNA. When EDTA is included in the AO staining buffer to remove Mg^{2+}, double-stranded RNA denatures, while DNA, which is more stable, is left double stranded (53). When

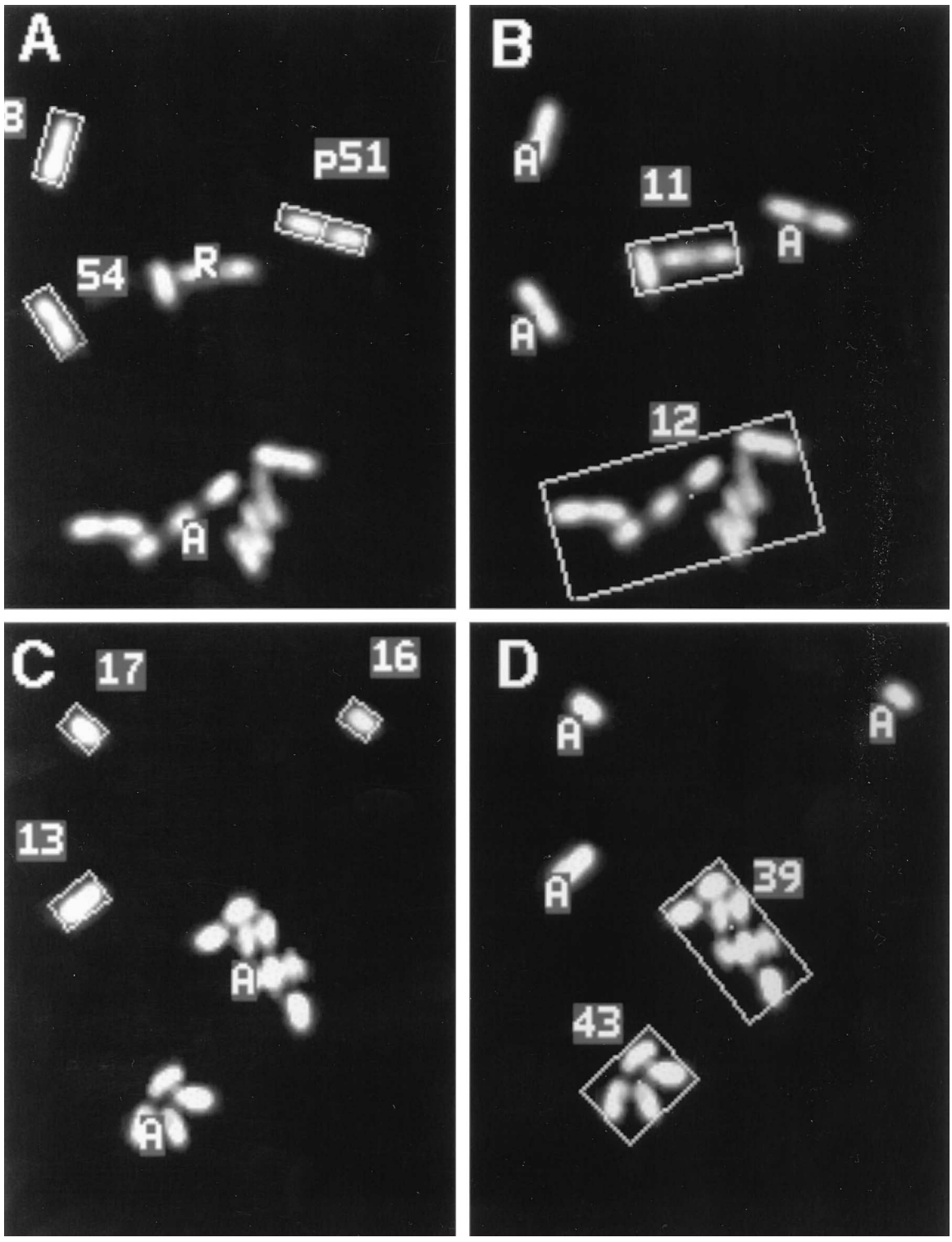

FIG. 1. Automatic identification of bacteria with Cellstat. (Upper panels) Results of an analysis of an image of exponentially growing *P. putida* KT2442 cells hybridized with a rhodamine-labelled ribosomal probe (Eub338). The image contains single cells as well as cell clumps. (A) The following parameters were used for identification of single cells: cell area between 75 and 700 pixels and high stringency on shape parameters. (B) The same viewing area as for panel A but analyzed for cell aggregates with a different set of parameters: cell size between 350 and 700 pixels and low stringency on shape parameters. (Lower panels) Results of a differential analysis of a surface-associated population. (C) Identification of single cells (cell size between 75 and 175 pixels and high stringency on shape parameters). (D) Identification of microcolonies on the surface (cell size between 200 and 7,000 pixels and low stringency on shape parameters). The boxes around the cells are not the actual cell edges defined by Cellstat, but they indicate the object-oriented bounding boxes of the cells, which were analyzed. A, cells outside the area limits defined; R, cells with an irregular shape; p, cell identified as dividing. The numbers refer to a list of data for each measured cell.

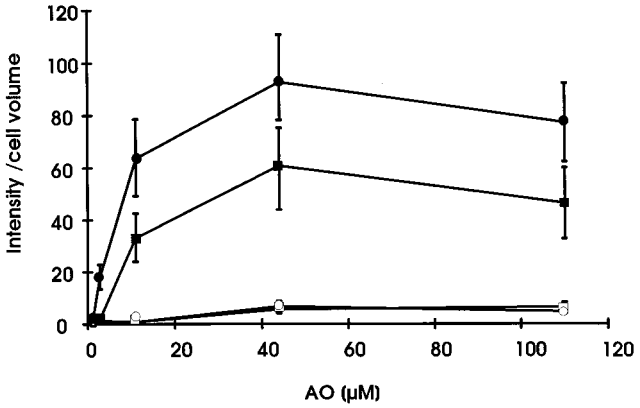

FIG. 2. *P. putida* KT2442 stained with increasing concentrations of AO. Results for a batch culture (●) with a doubling time of 0.9 h and a chemostat culture (■) with a dilution rate corresponding to a doubling time of 3.8 h are shown. Error bars indicate standard deviations between cells in a sample. ○ and □, the same cultures (doubling times of 0.9 and 3.8 h, respectively) but treated with RNase before AO staining.

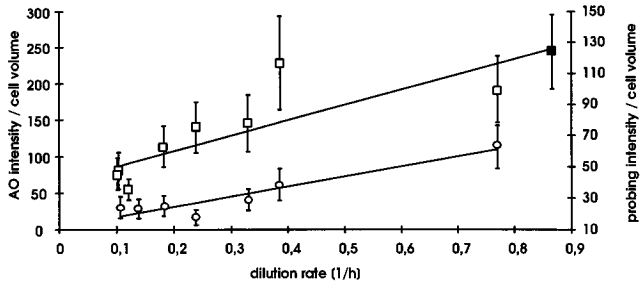

FIG. 3. RNA content of *P. putida* KT2442 at different growth rates. The RNA content was estimated by hybridization with the eubacterial probe EUB338 labelled with CY5 (○) and by AO staining (□). Cells were grown in a carbon-limited chemostat with different dilution rates. ■, an exponential batch culture stained with AO. The solid lines are regression lines for AO staining and 16S hybridization, respectively. The regression line for AO staining showed a correlation of $r^2 = 0.72$, and for the 16S hybridization the correlation was $r^2 = 0.89$. For both lines the linearity was highly significant ($P < 0.005$). Error bars indicate standard deviations (between 20 and 30%) among individual cells in a sample.

filter set XF21 (BP635/55) is used on the microscope, only the light emitted from AO bound to single-stranded nucleic acid—in this case RNA—is monitored. Since the majority (80 to 85%) of cellular RNA is rRNA (6), AO may be used as a ribosomal stain. To test this theory, exponentially growing cells of *P. putida* KT2442 were stained with different concentrations of AO under RNA-denaturing conditions. The staining intensity was measured by quantifying the amount of light emitted from stained single cells by image analysis as described in Materials and Methods. From Fig. 2 it is seen that an AO concentration of approximately 45 μM saturates the RNA. Higher concentrations seem to decrease the signal intensity, probably because of a change in the emission spectra for high AO/nucleic acid ratios, as mentioned by McFeters et al. (35). When RNase was added to whole cells prior to AO treatment, no signal was detected (Fig. 2), indicating that the light detected is specific for RNA. Furthermore, staining of cells growing with doubling times of 0.9 and 3.8 h, respectively, suggests that the RNA staining intensity is dependent on the RNA content of the cells and that it may be used as a growth rate indicator (Fig. 2). AO staining of the RNA in cells growing with different doubling times shows the same saturation kinetics independent of the growth rate (Fig. 2). Since AO has been shown to stain RNA in intact ribosomes (19), this suggests that the rRNA in ribosomes is equally accessible for staining in fast-growing and slowly growing cultures of *P. putida* KT2442.

Determination of growth rate-related parameters. To evaluate the possibility of using the intensity of AO staining as a growth rate indicator, *P. putida* KT2442 was grown in a carbon-limited chemostat at different dilution rates. The rRNA contents were estimated by hybridization with the 16S eubacterial probe EUB338; cells were visualized by epifluorescence microscopy, and digitized images were captured and subjected to image analysis. As can been seen from Fig. 3, the expected correlation between the rRNA content estimated by hybridization and the specific growth rate was observed. This is in accordance with earlier findings (11, 39) showing that it is possible to estimate the rRNA contents of single cells by hybridization with ribosomal probes and that the rRNA content correlates with the growth rate. Samples from the same chemostat cultures were also stained with AO, and the staining intensity was measured. The correlation between AO staining intensity and growth rate (Fig. 3) indicates that AO staining can be performed quantitatively, thereby allowing estimation of growth rates. The slope of the regression line for the AO staining is about three times larger than the slope for the 16S hybridization regression line. This can be explained by the fact that AO stains all types of single-stranded nucleic acid and accordingly measures all amounts of rRNA (including 23S rRNA), tRNA, and mRNA.

AO bound to double-stranded nucleic acid can be visualized using filter set 10 (42). In this way the DNA content of a single cell can be measured as the total amount of fluorescence from the cell, corresponding to the number of chromosomes in the cell. Figure 4 shows AO staining of *P. putida* KT2442 analyzed for DNA content. As can be seen, the DNA content was approximately doubled when the generation time was lowered from 6.8 h ($D = 0.10\ h^{-1}$) to 0.9 h ($D = 0.77\ h^{-1}$). This was in agreement with the results of flow cytometric analysis of the chromosomal contents of *P. putida* KT2442 cells grown in chemostat cultures, which showed an increase from 1.5 to 3.1 chromosomes per average cell when the generation time was changed from 6.8 to 0.9 h (Fig. 4). The flow cytometer gives quantitative measurements of chromosomal contents (51), and therefore we conclude that staining with AO provides the possibility to estimate both the RNA and the DNA contents of individual cells by simultaneous staining. AO staining has previously been used as an indicator of the physiological state of *E. coli* on the basis of the color of cells stained by the AO direct count method (3, 35). In contrast, the method presented here

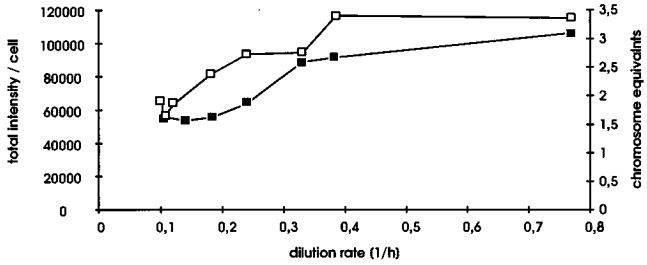

FIG. 4. DNA content of *P. putida* KT2442 at different growth rates as measured by AO staining (□) and flow cytometry (■). The various growth rates were obtained by growing *P. putida* KT2442 in a carbon-limited chemostat with different dilution rates. The fluorescence levels for the different cell populations measured with the flow cytometer were normalized to the fluorescence level for a starved culture containing one chromosome (see Materials and Methods) to give the average number of chromosomes in the culture.

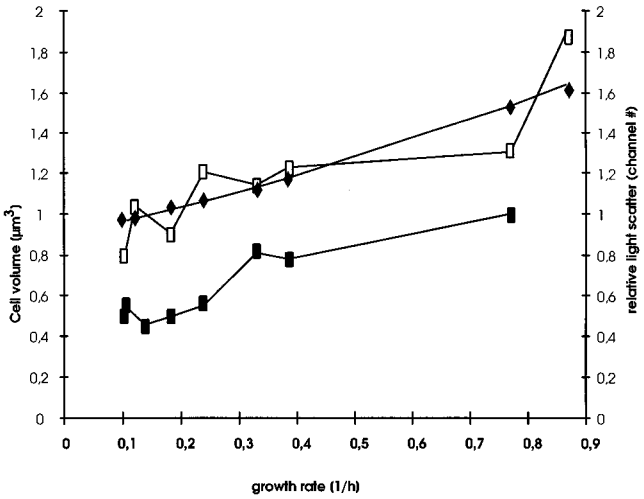

FIG. 5. Cell size of *P. putida* KT2442 at different growth rates. Cell volumes measured with Cellstat are indicated by open boxes, and the theoretical relationship [$V = V_0 e^{(\mu \ln 2)}$] originally found for *E. coli* is denoted by diamonds. For the best fit V_0 was estimated to be 0.9 μm^3. Light scatter measurements obtained with the flow cytometer are indicated by solid boxes. Volumes were calculated by assuming that 1 μm corresponded to 9.264 pixels. The various growth rates were obtained by growing cells in a carbon-limited chemostat with different dilution rates.

separates emission from AO bound to cellular RNA and emission from AO bound to DNA, allowing quantification of the cellular contents of both types of macromolecules.

AO staining and 16S hybridization techniques for estimating the physiological state of bacteria are based on the correlation between growth rate and macromolecular content. However, under conditions such as starvation, during which bacteria contain a much reduced number of ribosomes (16, 21), such a relationship becomes meaningless. Therefore, parameters like the cell volume or the FDC are needed to infer the physiological states of bacteria in environmental samples.

The volume (V) of *E. coli* is known to increase exponentially with the growth rate according to the following equation (13):

$$V = V_0 e^{(\mu \ln 2)} \quad (1)$$

where μ is the specific growth rate and V_0 corresponds to a hypothetical cell volume at $\mu = 0\ h^{-1}$. For *E. coli* V_0 is 0.4 μm^3 (13). By using image analysis to circumscribe cells, the volume of *P. putida* KT2442 could be correlated with the growth rate as shown in Fig. 5. A close agreement between the experimentally obtained values and the curve for the mathematical relation between volume and growth rate (equation 1) is obtained if V_0 is set at 0.9 μm^3 (Fig. 5). This corresponds to the size of cells of *P. putida* KT2442 starved for carbon for 8 h (data not shown). In addition, light scatter measurements obtained by using the flow cytometer, which are known to be a good indicator of cell size (5), showed that the cell size doubled over the range of growth rates tested (Fig. 5). This corresponds to the doubling of the cell volume found by image analysis.

Another measurable growth rate-related parameter is the FDC, which has previously been used to estimate growth rates in natural populations (23). By using image analysis, dividing cells in a population can be identified (Fig. 1A), and the FDC may serve as an independent measure of the physiological state in situ. Visual inspection of analyzed digitized images indicated that a reasonable setting of the discriminator for detection of dividing cells was 0.86, i.e., a cell was classified as dividing if a profile of the intensity projected on the main axis of the cell showed a minimum of 14% less intensity than the cell maximum. Figure 6 shows the FDCs estimated by image analysis for chemostat cultures of *P. putida* KT2442 grown with different dilution rates. As can be seen, a larger fraction of dividing cells is detectable in fast-growing cultures than in more slowly growing cultures. Linear regression ($r^2 = 0.69$; $P < 0.001$) indicates that the FDC is growth rate dependent, as found for natural bacterial populations (23). A theoretical correlation between the FDC and growth rates is included in Fig. 6. This FDC estimate is based on the mitotic index determined for eukaryotic cells (48), and it gives the fraction of cells in an exponential culture engaged in mitosis, i.e., cell division. The relation for an exponentially growing culture is as follows: $FDC = e^{\tau\mu} - 1$, where τ is the fraction of the cell cycle needed for the constriction leading to cell division. For values of the product $\mu\tau$ smaller than 1, which are physiologically relevant, a mathematical Taylor series expansion shows that there is an approximate linearity between the FDC and the specific growth rate, as indicated in Fig. 6. For *E. coli* the constriction time has been estimated to be 10 min at high growth rates (59), but it is dependent on the growth rate in the case of slowly growing cultures. For simplicity the constriction time for *P. putida* KT2442 was assumed to be constant (τ = 10 min), and this resulted in a simulation that corresponds well with the experimental findings (Fig. 6). In the starvation situation, in which μ is close to 0, the model predicts no dividing cells, whereas the experimental findings indicate about 6% dividing cells at μ = 0. An analysis of samples from cultures of *P. putida* KT2442 starved for 1 to 3 days showed that 6.7% of the population consisted of dividing cells. After 1 day of starvation, *P. putida* KT2442 would have undergone reductive divisions (21) and no dividing cells would be expected, and so the 6% dividing cells indicated by extrapolation of the regression line to μ = 0 probably corresponds to cells accidentally clumped together on the microscope slide.

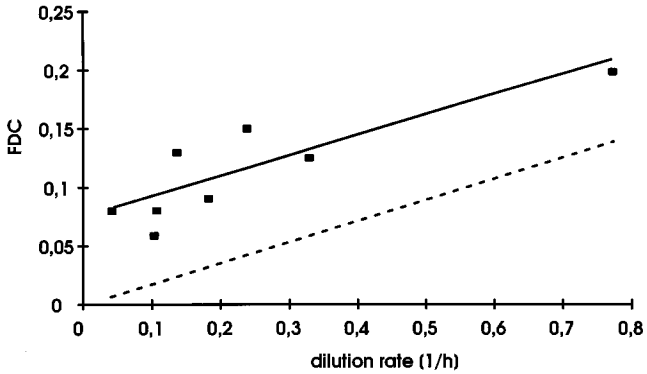

FIG. 6. FDC of *P. putida* KT2442 at different growth rates. ■, FDC as determined by image analysis. The solid line is a plot of the regression line for the set of data ($r^2 = 0.75$; $P < 0.01$). Data are averages of results for six images corresponding to between 500 and 800 cells. The broken line indicates a theoretical dependence of the FDC on the growth rate, as determined by using the mitotic index (48). To calculate the FDC from the model the constriction time (τ) was set at 10 min. The various growth rates were obtained by growing *P. putida* KT2442 in a carbon-limited chemostat with different dilution rates.

Direct estimates of growth rates on glass surfaces. The array of growth rate-related parameter determinations described above was used to compare the physiological states of surface-associated and planktonic growing cells under similar growth conditions. A small chemostat was constructed, and after growth for approximately 10 generations, a glass surface (a coverslip) was placed into the chemostat. Surface growth on the coverslip was allowed to develop for 14 to 20 h, resulting in a single layer of surface-attached cells. Subsequently, samples were withdrawn from the planktonic population and the sur-

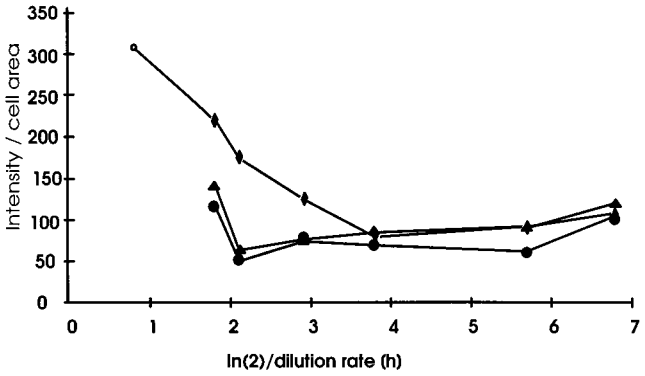

FIG. 7. Hybridization of planktonic and surface-associated cells sampled from cultures grown in a chemostat operated at different dilution rates. Hybridization intensities per cell area for planktonic cells (◆) and for surface-associated populations of *P. putida* KT2442 (●, single cells; ▲, microcolonies) are shown. ○, an exponential batch culture included for comparison. The *x*-axis label (ln2 divided by the dilution rate of the chemostat) corresponds to the doubling time for cells in the liquid phase. Cells were hybridized with bacterial probe EUB338 labelled with CY3.

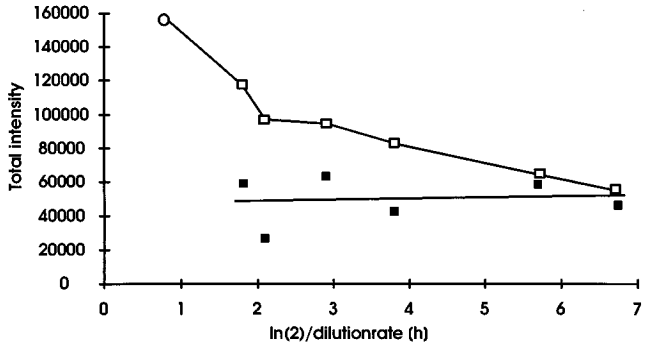

FIG. 8. DNA contents of planktonic and surface-associated cells in cultures grown in a chemostat operated at different dilution rates. The planktonic population (□) and the surface-attached population (■) were stained with AO and visualized to determine their DNA content. ○, an exponential batch culture included for comparison. The *x*-axis label (ln2 divided by the dilution rate of the chemostat) corresponds to the doubling time for cells in the planktonic phase.

face-attached population and fixed for hybridization, and the staining intensities of the two populations were compared. By varying the dilution rate of the chemostat, various growth rates of the planktonic population were supported.

Figure 7 shows the results of 16S rRNA hybridizations of samples from the planktonic and substratum-associated populations from chemostat cultures grown at various dilution rates. The cell intensities per cell area, which allow estimates of mean intensities of cell aggregates such as microcolonies, are shown. Cells in the liquid phase reduced their rRNA contents with increasing doubling time, i.e., at low dilution rates in the chemostat (Fig. 7). The surface population was analyzed with respect to single cells and microcolonies, as these populations could be distinguished by image analysis (Fig. 1C and D). In contrast to cells in the planktonic phase, the substratum-associated population showed a relatively constant hybridization intensity over the range of dilution rates tested, indicating a maximum doubling time of approximately 4 h (Fig. 7). The constant RNA contents of the surface-attached population were confirmed by AO staining of the two populations for RNA content (data not shown).

In addition, the DNA contents of single cells on the surface and in the liquid phase were determined by AO staining (Fig. 8). The measured DNA content of substratum-attached cells was rather uniform, in accordance with the constant physiological state of the surface-attached population, as inferred from RNA measurements. Furthermore, a constant cell volume (approximately 1.1 μm^3) was measured for the surface-attached population, whereas the volume of the planktonic population decreased as seen in Fig. 5. This further supported the constant physiological state of cells attached to the surface. Estimates of the number of dividing cells showed a decreasing FDC for the planktonic population when the chemostat dilution rate was lowered (as seen in Fig. 6) and a constant FDC for the surface-associated population (data not shown), again indicating a constant physiological state for cells attached to the surface. The FDC on the surface was in the range of 20 to 25%, somewhat higher than the 20% measured for an exponential batch culture with a doubling time of 0.9 h. The high FDC for the surface population may have been an artifact caused by cells that divided at the surface but were not spatially separated following cell division.

DISCUSSION

Studies of the growth physiology of bacteria have been performed almost exclusively with monocultures of cells suspended in liquid media of known composition and under conditions controllable by the investigator. In this way a very large amount of valuable information concerning a few model organisms has been accumulated over the years. Patterns of synthesis of macromolecules such as DNA, RNA, and proteins have been the basis for developing our present-day understanding of the controlled life activities of bacteria and their reactions to changing environments. The great advantages of studying cell suspensions under conditions of balanced, exponential growth (in addition to the important correlations revealed) is the reproducibility and predictability of such experiments, and for quantitative biology these features of the experiments are highly important.

In natural environments, however, bacteria do not grow exponentially (except for short periods), and more importantly they do not normally grow in suspension. Obviously, polluted waters will support planktonic microbial growth to fairly high cell densities, but in general bacteria are most active (9, 55) and present at the highest densities on surfaces, where the concentration of nutrients presumably is highest. In order to understand bacterial physiology in natural environments, it therefore becomes necessary at some point to address surface-bound populations and to investigate the physiologically relevant cellular parameters as revealed by test-tube experiments. We have initiated such an enterprise, and by combining the information on bacterial physiology obtained from exponentially growing cultures with sophisticated and very specific molecular techniques for single-cell analysis, we hope to be able to shed some light on bacterial life and activity in situ.

Surface-associated organisms in natural communities are believed to be more active than their planktonic counterparts, and this has been attributed to the accumulation of nutrients at the surface (9, 17, 24, 25, 28, 32, 55, 61). However, there have been reports of equal or higher levels of activity for the planktonic population (7, 18, 52). To investigate the growth of sessile and planktonic cell populations, growth rate-related parameters were determined for samples from a chemostat which supported growth of both planktonic and substratum-attached cell populations. Both types of cell populations were analyzed by 16S ribosomal probe hybridization, by AO staining for cellular RNA and DNA contents, by cell volume measurements, and by FDC estimates (Fig. 7 and 8 and data not shown). All

growth parameters showed the same overall trend: growth of the planktonic population correlated well with the dilution rate of the chemostat, whereas growth parameters measured for cells associated with the surface were independent of the dilution rate. This indicates that on the surface a constant cellular physiological state is quite rapidly established regardless of the dilution rate in the chemostat. The data for *P. putida* KT2442 suggest that when growth in the liquid phase is suboptimal because of a limited nutrient supply, growth on surfaces competes well with that in the planktonic population, making surface attachment favorable. Under conditions of ambient nutrient supply the situation is the opposite.

A relatively simple explanation for the observed constancy of the physiological state of the surface-bound bacteria is that they encounter a constant nutrient concentration. By assuming Monod kinetics for growth of the planktonic population, the basic chemostat equations show that the substrate concentration in the liquid medium is dependent on the dilution rate (22). This indicates that the surface population is exposed to a different nutrient environment than the planktonic population. The primary source of nutrients for the surface-bound bacteria could be organic molecules bound to the glass surface (the substratum); this layer of molecules is probably quite constant, being mainly determined by the surface properties and the nature of the nutrient molecules rather than the concentrations of nutrients (33). Thus, the constancy of the physiological state of the surface-attached cells observed here supports the notion of local environments for surface communities, and it also illustrates the usefulness of the applied molecular techniques as means of exposing such conditions.

As a tool for measuring growth rate-related parameters an image analysis program, Cellstat, which circumscribes cells in a digitized image of a hybridized or stained cell population has been developed. Cells are circumscribed by expanding cell size from the cell-intensity maximum in a smoothed version of the image to an isointensity level which corresponds to 20% of the intensity maximum (default setting), thereby defining a cell edge. This provides a reproducible and intensity-independent way of defining the cell (data not shown), and it is clearly an improvement over edge detection defined by the operator by manual circumscribing. The second derivative method for optimal edge detection has been applied for detection of picoplankton, but as stated by Viles and Sieracki (56), this method needs modification for application to larger cells.

On the basis of the automatic circumscription, quantitative measurements of single-cell staining intensities, cell size (volume), and the FDC for a population can be performed. This allows computation of RNA and DNA staining intensities, which are related to the growth rate (Fig. 3 and 4). For calculation of cell volume a mathematical three-dimensional reconstruction of the two-dimensionally projected cell is performed. Cells are assumed to be straight, and the volume is determined by integrating slices of revolution along the main axis of the cell. This method is similar to that used by Sieracki et al. (47). This iterative algorithm gives a very reliable approximation of the volumes of cells with septa, and it is an improvement over the common geometrical assumption that cells are cylinders with spheres at each end (29). Cell sizes calculated from digitized images show that the volume of *P. putida* KT2442 is dependent on its growth rate (Fig. 5), suggesting that the cell size of this organism can be used as an indicator of its growth rate. FDC is another cell shape parameter that can been related to the growth rate of the population (23). By using image analysis, a dividing cell is identified (Fig. 1A) as a cell having a minimum of a defined magnitude in the cross-sectional intensity profile along the central axis of the cell, and this intensity minimum will correspond to the septum in the dividing cell. The FDCs determined for *P. putida* KT2442 at different growth rates were in accordance with model predictions (Fig. 6), indicating that the FDC measured by image analysis can be used as a parameter to estimate the growth rate of a bacterial population. Furthermore, the identification of dividing cells allows population growth rate estimates to be compared with estimates of the subpopulation of cells which are actively growing (the dividing cells).

To supplement the growth rate estimates based on macromolecular (rRNA) content, a method was developed to determine the RNA/DNA ratio for single cells, since this ratio is growth rate dependent (14, 26). The method is based on AO staining of the nucleic acids, and it takes advantage of differential emission spectra of AO bound to single- and double-stranded nucleic acids (42). For *P. putida* KT2442 the RNA and DNA contents were shown to be related to the growth rate (Fig. 3 and 4), and accordingly the RNA/DNA ratio could be calculated (data not shown).

Investigations of environmental samples of microorganisms analogous to those described here for the chemostat samples may yield hitherto-inaccessible information about the life of bacteria in their natural habitats. With species-specific tools such as rRNA oligonucleotide probes it is possible to identify and characterize one organism at a time, independently of the complexity of the community, and once they are defined by such markers other parameters, such as DNA content, cell size, the division index, etc., may be recorded with the proper tools for the very same cells. It is important to emphasize, however, that bacteria present in such environmental samples do not necessarily grow exponentially. Therefore, the measurements of the growth-related parameters described above will provide information about the physiological state of the cells, i.e., cell shape and cell composition. To convert this information into estimated growth rates is impossible, since in most cases the growth of individual cells follows complex patterns. Nevertheless, by defining experimentally the physiological state of the cells, two important pieces of information become available: (i) an apparent maximum growth rate obtainable at the sampling time and (ii) a reflection of the local environment "seen" by the cell.

In conclusion, we have developed an image analysis program, Cellstat, which together with macromolecular staining allows the estimation of a variety of independent growth rate-related parameters, such as cellular RNA and DNA contents, cell volume, and the FDC of a bacterial population. The automated image analysis is not biased by the operator, and it allows the analysis of a number of objects, ensuring good statistics. We have shown here how these techniques for estimating the cellular physiological state may be applied to surface-attached organisms. Taken together, measurements of this pool of growth rate-related parameters provide the tools needed to investigate bacterial physiology in situ in multispecies, surface-associated communities.

REFERENCES

1. **Amann, R. I., L. Krumholz, and D. A. Stahl.** 1990. Fluorescent-oligonucleotide probing of whole cells for determinative, phylogenetic, and environmental studies in microbiology. J. Bacteriol. **172:**762–770.
2. **Amann, R. I., J. Stromley, R. Devereux, R. Key, and D. A. Stahl.** 1992. Molecular and microscopic identification of sulfate-reducing bacteria in multispecies biofilms. Appl. Environ. Microbiol. **58:**614–623.
3. **Back, J. P., and R. G. Kroll.** 1991. The differential fluorescence of bacteria stained with acridine orange and the effects of heat. J. Appl. Bacteriol. **71:**51–58.
4. **Bjørnsen, P. K.** 1986. Automatic determination of bacterioplankton biomass by image analysis. Appl. Environ. Microbiol. **51:**1199–1204.
5. **Boye, E., H. B. Steen, and K. Skarsted.** 1983. Flow cytometry of bacteria. J. Gen. Microbiol. **129:**973–980.

6. **Bremer, H., and P. P. Dennis.** 1987. Modulation of chemical composition and other parameters of the cell cycle by growth rate, p. 1527–1542. *In* F. C. Neidhardt, J. L. Ingraham, K. B. Low, B. Magasanik, M. Schaechter, and H. E. Umbarger (ed.), *Escherichia coli* and *Salmonella typhimurium*: cellular and molecular biology. American Society for Microbiology, Washington, D.C.
7. **Caldwell, D. E., and J. R. Lawrence.** 1986. Growth kinetics of *Pseudomonas fluorescens* microcolonies within the hydrodynamic boundary layers of surface microenviroments. Microb. Ecol. **12:**299–312.
8. **Clark, J. D., and O. Maaløe.** 1967. DNA replication and the cell cycle in *Escherichia coli* cells. J. Mol. Biol. **23:**99–112.
9. **Costerton, J. W., K.-J. Cheng, G. G. Geesey, T. I. Ladd, J. C. Nickel, M. Dasgupta, and J. T. Marrie.** 1987. Bacterial biofilms in nature and disease. Annu. Rev. Microbiol. **42:**435–464.
10. **Costerton, J. W., A. Lewandowski, D. DeBeer, D. Caldwell, D. Korber, and G. James.** 1994. Biofilms, the customized microniche. J. Bacteriol. **176:**2137–2142.
11. **DeLong, E. F., G. S. Wickham, and N. R. Pace.** 1989. Phylogenetic stains: ribosomal RNA-based probes for identification of single cells. Science **243:** 1360–1362.
12. **de Lorenzo, V., E. Linsay, B. Kessler, and K. T. Timmis.** 1993. Analysis of *Pseudomonas* gene products using *lac^{q}IPtrp-lac* plasmids and transposons that confer conditional phenotypes. Gene **123:**17–24.
13. **Donachie, W. D., and A. C. Robinson.** 1987. Cell division: parameter values and the process, p. 1578–1593. *In* F. C. Neidhardt, J. L. Ingraham, K. B. Low, B. Magasanik, M. Schaechter, and H. E. Umbarger (ed.), *Escherichia coli* and *Salmonella typhimurium*: cellular and molecular biology. American Society for Microbiology, Washington, D.C.
14. **Dortch, Q., T. L. Roberts, J. R. Clayton, Jr., and S. I. Ahmed.** 1983. RNA/DNA ratios and DNA concentrations as indicators of growth rate and biomass in planktonic marine organisms. Mar. Ecol. Prog. Ser. **13:**61–71.
15. **Dubuisson, M., A. K. Jain, and M. K. Jain.** 1994. Segmentation and classification of bacterial culture images. J. Microbiol. Methods **19:**279–295.
16. **Flärdh, K., P. S. Cohen, and S. Kjelleberg.** 1992. Ribosomes exist in large excess over the apparent demand for protein synthesis during carbon starvation in marine *Vibrio* sp. strain CCUG 15956. J. Bacteriol. **174:**6780–6788.
17. **Fletcher, M.** 1979. A microautoradiographic study of the activity of attached and free-living bacteria. Arch. Microbiol. **122:**271–274.
18. **Fletcher, M.** 1986. Measurement of glucose utilization by *Pseudomonas fluorescens* that are free-living and that are attached to surfaces. Appl. Environ. Microbiol. **52:**672–676.
19. **Furano, A. V., D. F. Bradley, and L. G. Childers.** 1966. The conformation of the ribonucleic acid in ribosomes. Dye stacking studies. Biochemistry **5:** 3044–3056.
20. **Giovannoni, S. J., E. F. DeLong, G. J. Olsen, and N. R. Pace.** 1988. Phylogenetic group-specific oligodeoxynucleotide probes for identification of single microbial cells. J. Bacteriol. **170:**720–726.
21. **Givskov, M., L. Eberl, S. Møller, L. K. Poulsen, and S. Molin.** 1994. Responses to nutrient starvation in *Pseudomonas putida* KT2442: analysis of general cross-protection, cell shape, and macromolecular content. J. Bacteriol. **176:**7–14.
22. **Gottschal, J. C., and L. Dijkhuizen.** 1988. The place of the continuous culture in ecological research, p. 19–49. In J. W. T. Wimpenny (ed.), CRC handbook of laboratory model systems for microbial ecosystems. CRC Press, Inc., Boca Raton, Fla.
23. **Hagström, Å., U. Larsson, P. Hörstedt, and S. Normark.** 1979. Frequency of dividing cells, a new approach to the determination of bacterial growth rates in aquatic environments. Appl. Environ. Microbiol. **37:**805–812.
24. **Hendricks, C. W.** 1974. Sorption of heterotrophic and enteric bacteria to glass surfaces in the continuous culture of river water. Appl. Microbiol. **28:**572–578.
25. **Kefford, B., S. Kjelleberg, and K. C. Marshall.** 1982. Bacterial scavenging: utilization of fatty acids localized at a solid liquid interface. Arch. Microbiol. **133:**257–260.
26. **Kemp, P. F., S. Lee, and J. LaRoche.** 1993. Estimating the growth rate of slowly growing marine bacteria for RNA content. Appl. Environ. Microbiol. **59:**2594–2601.
27. **Kjeldgaard, N. O., and C. G. Kurland.** 1963. The distribution of soluble and ribosomal RNA as a function of growth rate. J. Mol. Biol. **6:**341–348.
28. **Kjelleberg, S., B. A. Humphery, and K. C. Marshall.** 1982. Effects of interfaces on small starved marine bacteria. Appl. Environ. Microbiol. **43:**1166–1172.
29. **Krambeck, C., H. Krambeck, and J. Overbeck.** 1981. Microcomputer-assisted biomass determination of plankton bacteria on scanning electron micrographs. Appl. Environ. Microbiol. **42:**142–149.
30. **Krogfelt, K. A., L. K. Poulsen, and S. Molin.** 1993. Identification of coccoid *Escherichia coli* BJ4 cells in the large intestine of streptomycin-treated mice. Infect. Immun. **61:**5029–5034.
31. **Lawrence, J. R., D. R. Korber, B. D. Hoyle, J. W. Costerton, and D. E. Caldwell.** 1991. Optical sectioning of microbial biofilms. J. Bacteriol. **173:** 6558–6567.
32. **Manz, W., U. Szewzyk, P. Ericsson, R. Amann, K.-H. Schleifer, and T.-A. Stenström.** 1993. In situ identification of bacteria in drinking water and adjoining biofilms by hybridization with 16S and 23S rRNA-directed fluorescent oligonucleotide probes. Appl. Environ. Microbiol. **59:**2293–2298.
33. **Marshall, K. C.** 1986. Adsorption and adhesion processes in microbial growth at interfaces. Adv. Coll. Interface Sci. **25:**59–86.
34. **Marshall, K. C.** 1992. Biofilms: an overview of bacterial adhesion, activity, and control at surfaces. ASM News **58:**202–207.
35. **McFeters, G. A., A. Singh, S. Byun, P. R. Callis, and S. Williams.** 1991. Acridine orange staining reaction as an index of physiological activity in *Escherichia coli*. J. Microbiol. Methods **13:**87–97.
36. **Morgan, J. A. W., G. Rhodes, and R. W. Pickup.** 1993. Survival of nonculturable *Aeromonas salmonicida* in lake water. Appl. Environ. Microbiol. **59:**874–880.
37. **Neidhardt, F. C., and B. Magasanik.** 1960. Studies on the role of ribonucleic acid in the growth of bacteria. Biochim. Biophys. Acta. **42:**99–116.
38. **Pang, P., and H. H. Winkler.** 1994. The concentration of stable RNA and ribosomes in *Rickettsia prowazekii*. Mol. Microbiol. **12:**115–120.
39. **Poulsen, L. K., G. Ballard, and D. A. Stahl.** 1993. Use of rRNA fluorescence in situ hybridization for measuring the activity of single cells in young and established biofilms. Appl. Environ. Microbiol. **59:**1354–1360.
40. **Ramsing, N. B., M. Kühl, and B. B. Jørgensen.** 1993. Distribution of sulfate-reducing bacteria, O_2, and H_2S in photosynthetic biofilms determined by oligonucleotide probes and microelectrodes. Appl. Environ. Microbiol. **59:** 3840–3849.
41. **Raskin, L., L. K. Poulsen, D. R. Noguera, B. E. Rittmann, and D. A. Stahl.** 1994. Quantification of methanogenic groups in anaerobic biological reactors by oligonucleotide probe hybridization. Appl. Environ. Microbiol. **60:** 1241–1248.
42. **Rigler, R. J.** 1966. Microfluorometric characterization of intracellular nucleic acids and nucleoproteins by acridine orange. Acta Physiol. Scand. **67:**1–122.
43. **Rodrigues, G. G., D. Phipps, K. Ishiguro, and F. Ridgway.** 1992. Use of a fluorescent redox probe for direct visualization of actively respiring bacteria. Appl. Environ. Microbiol. **58:**1801–1808.
44. **Rosset, R., J. Juelien, and R. Monier.** 1966. Ribonucleic acid composition of bacteria as a function of growth rate. J. Mol. Biol. **18:**308–320.
45. **Schaechter, M., O. Maaløe, and N. O. Kjeldgaard.** 1958. Dependency on medium and temperature of cell size and chemical composition during balanced growth of *Salmonella typhimurium*. J. Gen. Microbiol. **19:**592–606.
46. **Sieracki, M. E., S. E. Reichenbach, and K. L. Webb.** 1989. Evaluation of automated threshold selection methods for accurately sizing microscopic fluorescent cells by image analysis. Appl. Environ. Microbiol. **55:**2762–2772.
47. **Sieracki, M. E., C. L. Viles, and K. L. Webb.** 1989. Algorithm to estimate cell biovolume using image analyzed microscopy. Cytometry **10:**551–557.
48. **Smith, C. L., and P. P. Dendy.** 1962. Relation between mitotic index, duration of mitosis, generation time and fraction of dividing cells in a cell population. Nature (London) **193:**555–556.
49. **Stahl, D. A., and R. I. Amann.** 1991. Development and application of nucleic acid probes, p. 205–248. *In* E. Stackebrandt and M. Goodfellow (ed.), Nucleic acid techniques in bacterial systematics. John Wiley and Sons, New York.
50. **Stahl, D. A., B. Flesher, H. R. Mansfield, and L. Montgomery.** 1988. Use of phylogenetically based hybridization probes for studies of ruminal microbial ecology. Appl. Environ. Microbiol. **54:**1079–1084.
51. **Steen, H. B.** 1983. A microscope-based flow cytophotometer. Histochem. J. **15:**147–160.
52. **Szewzyk, U., and B. Schink.** 1988. Surface colonization by and life cycle of *Pelobacter acidigallici* studied in a continuous-flow microchamber. J. Gen. Microbiol. **134:**183–190.
53. **Traganos, F., T. Darzynkiewicz, and M. R. Melamed.** 1977. Simultaneous staining of ribonucleic and deoxyribonucleic acids in unfixed cells using acridine orange in a flow cytometric system. J. Histochem. Cytochem. **25:**46–56.
54. **Tsien, H. C., B. J. Bratina, K. Tsuji, and R. S. Hanson.** 1990. Use of oligodeoxynucleotide signature probes for identification of physiological groups of methylotrophic bacteria. Appl. Environ. Microbiol. **56:**2858–2865.
55. **van Loosdrecht, M. C. M., J. Lyklema, W. Norde, and A. J. B. Zehnder.** 1990. Influence of interfaces on microbial activity. Microbiol. Rev. **54:**75–87.
56. **Viles, C. L., and M. E. Sieracki.** 1992. Measurement of marine picoplankton cell size by using a cooled charge-coupled device camera with image-analyzed fluorescent microscopy. Appl. Environ. Microbiol. **58:**584–592.
57. **Ward, D. M., M. M. Bateson, R. Weller, and A. L. Ruff-Roberts.** 1992. Ribosomal RNA analysis of microorganisms as they occur in nature, p. 219–286. *In* K. C. Marshall (ed.), Advances in microbial ecology, Plenum Press, New York.
58. **Woese, C. R.** 1987. Bacterial evolution. Microbiol. Rev. **51:**221–271.
59. **Woldringh, C. L.** 1976. Morphological analysis of nuclear separation and cell division during the life cycle of *Escherichia coli*. J. Bacteriol. **125:**248–257.
60. **Zimmermann, R., R. Iturriaga, and J. Becker-Birk.** 1978. Simultaneous determination of the total number of aquatic bacteria and the number thereof involved in respiration. Appl. Environ. Microbiol. **36:**926–935.
61. **Zobell, C. E.** 1943. The effect of solid surfaces upon bacterial activity. J. Bacteriol. **46:**39–56.